Achievable Energy Efficiency in Massive MIMO: Impact of DAC Resolution and PAPR Reduction for Practical Network Topologies at mm-Waves

C.A. Schmidt, J. F. Schmidt, J. L. Figueroa, M. Crussiere

Achievable Energy Efficiency in Massive MIMO: Impact of DAC Resolution and PAPR Reduction for Practical Network Topologies at mm-waves

C. A. Schmidt, J. F. Schmidt, J. L. Figueroa, and M. Crussière

***Abstract*—This paper explores key parameters of a massive MIMO system and their impact on energy efficiency at transmission. In particular, the effect of the digital to analog converter resolution and peak to average power ratio reduction techniques are addressed, in the context of practical user location distributions for both line and non line of sight channels. Results show interesting design trade-offs, and highlight the relevance of an accurate model for the user locations for the correct evaluation of the achievable performance.**

I. Introduction

MASSIVE MIMO is considered a key technology to achieve the required data rate, bandwidth, and reliability in modern wireless communication systems such as 5G NR and beyond [1] [2]. The use of large antenna arrays ($N_T > 64$) in the base station (BS) allows for a significant increase in the signal to noise ratio (SNR), as well as spatial diversity transmission through narrow beams directed to specific locations [3]. Both features make millimeter wave communications feasible at the higher frequency band extending from 24 to 52 GHz [4]. Indeed, they turn out to be an effective manner to overcome the increased propagation path-loss conditions in the higher part of the spectrum [5] [6]. However, a large amount of antennas also means tougher hardware requirements due to the inscrease of the number of radio frequency (RF) chains, leading to higher power consumption [5]. In this sense, enhancement of the systems energy efficiency (EE) has become a major concern and focus of active research.

In general, EE in massive MIMO systems can be improved by either lowering the signal processing complexity and thus its associated power consumption, or by improving the hardware resources utilization[1] [7]. Following this criteria, a joint optimization of time domain beam-steering with peak-to-average power ratio (PAPR) reduction was proposed in [8] and [9], where computational complexity is significantly reduced while improving the power amplifier efficiency. Then, the actual gain in EE that can be obtained by PAPR reduction in a massive MIMO regime is analyzed in [10], where expressions of the EE and sum capacity are derived. However, that work considers users located at the same distance and far from the transmitter (200 m), which is a worst case scenario for the propagation path-loss.

In this paper, we analyze the impact of key system parameters on the EE of a massive MIMO system, accounting for more realistic user locations. In particular, we consider digital to analog converter (DAC) resolution and PAPR reduction which introduce interesting design trade-offs. For instance, higher DAC resolution improves the signal to quantization and noise ratio (SQNR) leading to higher throughput, but also increases the power consumption at the RF chains. On the other hand, PAPR reduction enhances the power-amplifier (PA) EE to the detriment of a higher power consumption at the DAC. Regarding the user locations, we consider a stochastic geometry model that captures three different network topologies. This model results in a very accurate characterization of the path-loss. As a result, better and more realistic results are expected when compared to [10]. The contributions of this work can be summarized as follows:

- The effect on the systems EE of DAC resolution and PAPR reduction are jointly modelled and analyzed. Then, this information can be exploited to define key system level parameters that maximize EE at transmission.
- The user location distribution is modelled by a stochastic geometry approach considering an inhomogeneous Poisson point process (PPP). This allows a detailed analysis of the systems EE for three scenarios: higher user density near the cell center, uniform distribution, and higher user density near the cell border.

The considered user location models represent the best, typical, and worst case scenarios, and are a realistic approximation to a real world realizations. They thus provide a reliable framework to accurately asses the effects of the studied parameters on the systems EE.

The remaining of this work is organized as follows. Section II presents the energy efficiency based on the user location distribution model, including the expressions for sum capacity, path-loss and power consumption. The effect of DAC resolution and PAPR reduction on power consumption, SNR and PA efficiency are presented in Section III. A numerical evaluation of the derived expressions is presented in Section IV, where the results are discussed. Finally, Section V concludes the paper.

C. A. Schmidt and J. L. Figueroa are with Instituto de Inv. en Ingeniería Eléctrica - CONICET/UNS, 8000 Bahía Blanca, Argentina (e-mails: cschmidt@uns.edu.ar, figueroa@uns.edu.ar).

J. F. Schmidt is with Institute of Networked and Embedded Systems - Alpen-Adria-Universität Klagenfurt, 9020 Klagenfurt, Austria (e-mail: jorge.schmidt@aau.at).

M. Crussière is with Univ. Rennes, INSA Rennes, IETR, UMR-CNRS 6164, 35000 Rennes, France (e-mail: matthieu.crussiere@insa-rennes.fr).

[1]The use of available hardware at the base station can be regulated to save energy when its not fully exploited (for example turning off a subset of transmit antennas on lower traffic), or optimized to improve efficiency in particular system components.

II. System model

In this section, we derive the expression for the sum capacity considering a stochastic geometry model for the user location distribution. Considering digital beamforming, a number of users U, and that each user can be located at a different distance d_u from the transmitter, which is a BS at the center of coordinates, the sum capacity $\bar{C}_{\Sigma D}$ can be rewritten as

$$\bar{C}_{\Sigma D} = W \sum_{u=1}^{U} \log_2 \left(1 + aP_L(d_u)\right), \tag{1}$$

where $P_L(d_u)$ is the distance-dependent path-loss, and we have introduced the term $a = (N_T P_{\text{PA}} \eta_{\text{PA}})/(WN_0 + N_Q)$ to get a more compact expression focused on the location model. Here W is the transmission bandwidth, U the number of users, and N_T the transmit antennas [10]. In addition, N_0 is the noise density, N_Q is the quantization noise, P_{PA} is the PA consumption, and η_{PA} the PA efficiency. Assuming a point process ϕ_u to model the users locations w.r.t. the transmitter, we can rewrite (1) as

$$\bar{C}_{\Sigma D} = W \sum_{i \in \phi_u} \log_2 \left(1 + aP_L(d_i)\right), \tag{2}$$

where the selected type of process ϕ_u will determine the network topology. Taking the expectation over the point process, we get

$$\bar{C}_{\Sigma D} = W \mathbb{E}_{\phi_u} \left\{ \sum_{i \in \phi_u} \log_2 \left(1 + aP_L(d_i)\right) \right\}. \tag{3}$$

Since the transmitter is at the origin, considering a user at coordinates (x, y) the distance of the link is $d = \|x, y\|$, and we can evaluate (3) in polar coordinates as

$$\bar{C}_{\Sigma D} = W \int_0^{2\pi} \int_0^{\infty} \log_2 \left(1 + aP_L(d)\right) f_d(d) \mathrm{d}d, \tag{4}$$

where $f_d(d)$ is the probability distribution function (pdf) of their distances to the BS. The solution to (4) will depend on the particular type of process that describes the network topology. Here, we consider an in-homogeneous PPP ϕ_u over a circular deployment of radius R around the BS, where the pdf of the distance is [11]

$$f_d(d) = \lambda_0 \left(1 + \kappa \left(d^2 - \frac{R^2}{2}\right)\right), \tag{5}$$

with $\kappa \in \left[-2/R^2, 2/R^2\right]$, and λ_0 the user density when ϕ_u is an homogeneous PPP. The expected number of users can be computed as $U = 2\pi \int_0^R d f_d(d) \mathrm{d}d$. Then, (4) becomes

$$\bar{C}_{\Sigma D} = \frac{W 4\pi\lambda_0}{R^2} \int_0^R \log_2 \left(1 + aP_L(d)\right) d \left(1 + \kappa \left(d^2 - \frac{R^2}{2}\right)\right) \mathrm{d}d. \tag{6}$$

Parameter κ defines three different scenarios. When $\kappa = 0$, the nodes are uniformly distributed around the BS; if $\kappa > 0$, there is higher concentration of users near the cell border; and finally $\kappa < 0$ means the user density is higher near the center of the circle, where the BS is. In order to solve (6), the integral can be separated in three parts as

$$\begin{aligned} \bar{C}_{\Sigma D} = {} & \frac{W 4\pi\lambda_0}{R^2} \int_0^R \log_2 \left(1 + aP_L(d)\right) d\mathrm{d}d \\ & + \frac{W 4\pi\lambda_0 \kappa}{R^2} \int_0^R \log_2 \left(1 + aP_L(d)\right) d^3 \mathrm{d}d \\ & - W 2\pi\lambda_0 \kappa \int_0^R \log_2 \left(1 + aP_L(d)\right) d\mathrm{d}d \end{aligned} \tag{7}$$

The path loss in mm-waves as a function of the distance d between transmitter and receiver can be modeled by [12]

$$P_L(d)[dB] = P_L(d_0) + \alpha 10 \log_{10}\left(d/d_0\right) + X \tag{8}$$

where $P_L(d_0)$ is the path loss in dB at free-space for a reference distance of d_0 (chosen to be 1 m), and α is the path-loss exponent. The term $X \sim N(0, \sigma_x)$ models the shadowing effect. The parameters α and σ_x are defined by the propagation conditions, and depend on the frequency of operation and type of link (LOS, NLOS, indoor, outdoor). Converting (8) from dB to Watts, we get $P_L(d_0) = 10 \log((4\pi d_0 f/c)^2)$, where f is the frequency of operation and c the speed of light; and $X = 10 \log_{10}(s)$, where s is the value in Watts of the shadowing factor. The attenuation of the signal at the receiver is then

$$P_L(d)[W] = [4\pi f/c)^2 s d^{\alpha}]^{-1} \tag{9}$$

Then, the integrals to solve are,

$$I_1 = \int_1^R d \log_2 \left(1 + Ad^{-\alpha}\right) \mathrm{d}d \tag{10}$$

$$I_2 = \int_1^R d^3 \log_2 \left(1 + Ad^{-\alpha}\right) \mathrm{d}d \tag{11}$$

where $A = a/(4\pi f/c)^2 s$, and the specific result will depend on the propagation conditions determined by the attenuation coefficient α. For example, assuming $\alpha = 2$ leads to

$$I_1 = \frac{(R^2 + A)\ln(R^2 + A) - 2R^2 \ln(R)}{2\ln(2)} - \frac{(1 + A)\ln(1 + A)}{2\ln(2)}$$

$$I_2 = \frac{(R^4 - A^2)\ln(R^2 + A) - 2R^4 \ln(R)}{4\ln(2)} - \frac{(1 - A^2)\ln(1 + A) - A(R^2 - 1)}{4\ln(2)}$$

Combinations of PPPs with different densities and κ parameters (as well as path-loss conditions) can also be considered by adding the corresponding integrals to (6). Thus, a variety of realistic deployment features can be captured by the formulation. In order to compute the energy efficiency η_{EE}, which is the ratio of the sum capacity $\bar{C}_{\Sigma D}$ and the total power consumption P_T, we can model P_T for digital beamforming by [10]

$$P_T = N_T(P_{\text{PA}} + P_{\text{RF}} + P_0) + P_{\text{common}}, \tag{12}$$

where $P_{\text{RF}} = P_{\text{DAC}} + P_{\text{M}}$ is the power consumption of each RF chain. Within the RF chain, P_{DAC} is the consumed power at the DAC, and P_{M} at the mixer. Finally, P_0 is a static power consumption dependent on the number of transceivers, and P_{common} is an additional static power consumption term.

III. Effect of DAC resolution and PAPR

A. Effect of DAC resolution on power consumption and SNR

DACs are key components of the individual RF chains that feed the signals to the antennas. DAC resolution affects many aspects of the system simultaneously. For instance, increasing the DAC resolution produces a higher SQNR because of the lower quantization noise, but it also increases the PAPR of the signal (which affects the PA efficiency) and leads to higher power consumption. As the energy efficiency is the ratio between the sum capacity and the power consumption, the effect of higher DAC resolution on the systems energy efficiency is difficult to predict.

We consider the current steering (CS) DAC architecture, which is widely used because it provides both high conversion speed and high resolution [13]. In this topology, the DAC is composed of several current sources, each connected to the same resistive load through a switch. The amount of current sources and their values depend on the way in which the input digital word is used to control the switches and generate the conversion. If a binary weight strategy is used to convert a B-bit digital word $W = [b_0, b_1, \cdots, b_{B-1}]$, then B current sources are used and their values are $I(b_i) = 2^i I_u$. Here, I_u is the unit of current that produces a voltage drop equivalent to a least-significant bit (LSB) on the resistive output load R_L. Then, the bits b_i are used to control the switches connected in series with the current sources, where the switches are turned off if $b_i = 0$, and turned on if $b_i = 1$, such that the output current for the binary weight scheme $I_{\text{out}}^{\text{BW}}$ is

$$I_{\text{out}}^{\text{BW}} = I_{\text{out}} = \sum_{i=0}^{B-1} b_i 2^i I_u. \tag{13}$$

which is the sum of the currents provided by the B current sources. Therefore, the analog output voltage from the DAC is $V_{\text{out}} = I_{\text{out}} R_L$, the output power is $P_{\text{out}} = I_{\text{out}}^2 R_L$, and the power consumption of the DAC analog circuitry can be computed as $P_{\text{DAC}}^A = I_{\text{out}} V_{\text{DD}}$, where V_{DD} is the supply voltage.

Another alternative is to use a segmented CS-DAC. In this case, the binary B-bit digital word is converted to a thermometric coded word of $B_T = 2^{B-1}$ bits, i.e., a bit for each possible equivalent analog voltage level. Here, there are B_T current sources with equal value I_u, each of them connected to a common resistive load R_L through a switch, such that the output current for the segmented scheme I_{out}^S is

$$I_{\text{out}}^S = I_{\text{out}} = \sum_{i=0}^{B_T-1} b_i I_u. \tag{14}$$

The advantage of a segmented CS-DAC is that it is very robust to circuit mismatches, in the sense that the transition between two consecutive voltage levels involve switching (on or off) only one current source. Its practical use, however, is limited to lower resolution DACs due to the exponential increase in the required amount of switches and current sources with B. A commonly used solution when low distortion and high resolution is needed consists on using a mixed architecture of partial segmentation. Indeed, a binary weighted structure can be used for the least significant bits of the input digital word, where linearity requirements can be relaxed. Conversely a segmented part can be used for the most significant bits (MSBs), where higher linearity is required as errors cause greater changes in the output voltage. As a result, the DAC quantization characteristic can be kept linear within a wide range of resolutions with reduced complexity. In this work we assume that partial segmentation is applied, such that the $B/2$ least significant bits are binary weighted and the rest use segmentation.

Consider now the power dissipation of the digital circuitry of the DAC. We assume that the power consumption is dominated by the switching operation, described by $P_{\text{DAC}}^D = \beta C_L f_{\text{clk}} V_{\text{DD}}^2$, where β is the average switching activity, f_{clk} is the clock frequency and C_L is the average load capacitance. Then, the total power consumption of the DAC is $P_{\text{DAC}} = P_{\text{DAC}}^A + P_{\text{DAC}}^D$. Note that P_{DAC}^D can be considered constant, while P_{DAC}^A is a function of the DAC resolution. In fact, we are interested in a direct relation between P_{DAC}^A and B.

Under these considerations, the output current of the partial segmentation DAC is

$$I_{\text{out}} = I_{\text{out}}^{MSB} + I_{\text{out}}^{LSB} = \sum_{i=B/2}^{B_{\max}} b_i 2^{B/2} I_u + \sum_{i=0}^{B/2-1} b_i 2^i I_u, \tag{15}$$

where $B_{\max} = 2^{B/2-1} + B/2 - 1$, and $2^{B/2} I_u$ is the unit current for the segmented MSBs. The maximum current will occur when all bits are set to one, that is $b_i = 1$, for all i,

$$I_{\max} = I_u \left(2^{B-1} + \sum_{i=0}^{B/2-1} 2^i \right) = I_u \left[2^{B-1} + 2^{B/2} - 1 \right].$$

Then the maximum signal power at the output of the DAC is $P_{\text{out,max}} = I_{\max}^2 R_L$. Considering a multi-carrier signal such as OFDM, the PAPR is,

$$\text{PAPR}|_{dB} = 10 \log \left(\frac{P_{\text{out,max}}}{\bar{P}_{\text{out}}} \right) = 20 \log \left(\frac{I_{\max}}{\bar{I}_{\text{out}}} \right). \tag{16}$$

Then, the average output current $\bar{I}_{\text{out}}$ can be computed as

$$\bar{I}_{\text{out}} = \frac{I_{\max}}{10^{\text{PAPR}|_{dB}/20}} = \frac{I_u \left[2^{B-1} + 2^{B/2} - 1 \right]}{10^{\text{PAPR}|_{dB}/20}}.$$

Therefore, the average analog power consumption is

$$P_{\text{DAC}}^A = \bar{I}_{\text{out}} V_{\text{DD}} = \frac{I_u \left[2^{B-1} + 2^{B/2} - 1 \right]}{10^{\text{PAPR}|_{dB}/20}} V_{DD},$$

which, considering a normalized bias voltage $V_{\text{DD}} = 1$ [V], leads to a total DAC power consumption of,

$$P_{\text{DAC}} = \frac{I_u \left[2^{B-1} + 2^{B/2} - 1 \right]}{10^{\text{PAPR}|_{dB}/20}} + \beta C_L f_{\text{clk}}. \tag{17}$$

Note that we are interested here in the dependence of the DAC power consumption on its resolution, while the actual accurate value may depend on the manufacturing process, technology and other factors negligible to our analysis.

For ADCs and DACs with resolution higher than four bits, the quantization noise can be modelled very accurately

following the usual assumption of white additive noise uniformly distributed in the rage $[-\Delta/2, \Delta/2]$ with variance $\sigma_Q^2 = \Delta^2/12$, where $\Delta = V_{\text{DD}}/2^B$ is the quantization step [14]. This enables adding this term as N_Q in the SNR expression (the term a in (1)) to evaluate its contribution on the energy efficiency of the system.

B. Effect of PAPR reduction

It was shown in [10] that adding PAPR reduction on a massive MIMO communications system can effectively increase its EE, regardless of the type of beamforming implemented (fully digital or hybrid). This is due to the improvement that can be obtained in the PA efficiency η_{PA}, as signals with lower PAPR can be amplified by PAs biased with a lower input back-off. However, the calculations assumed the worst case scenario where all users are far away from the base station, near the cell border. It should be expected that considering realistic spatial distributions for the users locations may give more accurate results. In addition, as shown in equation (17), a lower PAPR will also affect the power consumption at the DAC, which also has to be considered. In this section, we analyze how PAPR reduction affects the EE under this scenario.

The PA efficiency η_{PA} can be defined as

$$\eta_{PA} = \frac{\bar{P}_{PAo}}{P_{PA}} \tag{18}$$

where $\bar{P}_{PAo}$ is the average power of the signals at the output of the PA, while P_{PA} is the PA consumption. Considering a resistive load R_L to the PA, an average output current $\bar{I}_{PAo}$, and a suply voltage V_{DD}, we can aproximate $\bar{P}_{PAo} = (\bar{I}_{PAo})^2 R_L$ and $P_{PA} = \bar{I}_{PAo} V_{DD}$. Then, η_{PA} can be rewritten as

$$\eta_{PA} = \frac{(\bar{I}_{PAo})^2 R_L}{\bar{I}_{PAo} V_{DD}} = \bar{I}_{PAo} \frac{R_L}{V_{DD}} = \frac{\bar{I}_{PAo}}{I_{PA,max}} \tag{19}$$

where we replaced the maximum current at the otput of the PA $I_{PA,max} = V_{\text{DD}}/R_L$. From (16), we get

$$\eta_{PA} = 10^{-\text{PAPR}|_{dB}/20} \tag{20}$$

which we can use in the term a from (1) to evaluate the effect of PAPR on the systems energy efficiency.

Let us define the PA efficiency before and after PAPR reduction as $\eta_{PA_1} = 10^{-\text{PAPR}_1|_{dB}/20}$ and $\eta_{PA_2} = 10^{-\text{PAPR}_2|_{dB}/20}$. Considering $\text{PAPR}_2|_{dB} = \text{PAPR}_1|_{dB} - \Delta\text{PAPR}|_{dB}$, where $\Delta\text{PAPR}|_{dB}$ is the PAPR reduction, it is possible to rewrite $\eta_{PA_2} = \eta_{PA_1} 10^{\Delta\text{PAPR}|_{dB}/20}$. Then, we can define a gain in the PA efficiency due to PAPR reduction as $G = 10^{\Delta\text{PAPR}|_{dB}/20}$, such that $\eta_{PA_2} = G\eta_{PA_1}$.

IV. Numerical Evaluation

In this section we perform numerical evaluations of the derived expressions and discuss the results. We chose the following parameter values for the computation of the consumed power and the signal to quantization noise ratio (SQNR) that define the EE,

- $\eta_{\text{PA}} = 0.375$.
- $W = 200 \times 10^6$ [Hz].
- $N_0 = 1 \times 10^{-16}$ [W/Hz].

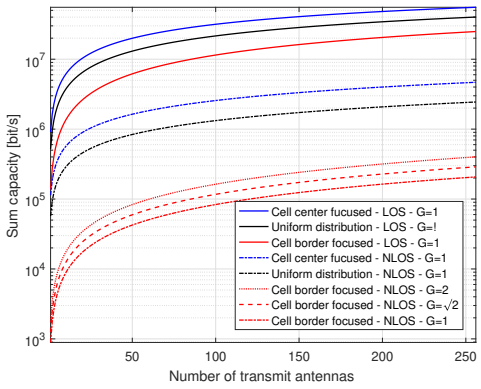

Fig. 1. Sum capacity for three different network topologies. The parameters used are: $\lambda_0 = 3$ [users/Km^2], $B = 12$, $\alpha = 2, 3$ (LOS, NLOS), $G = 1$.

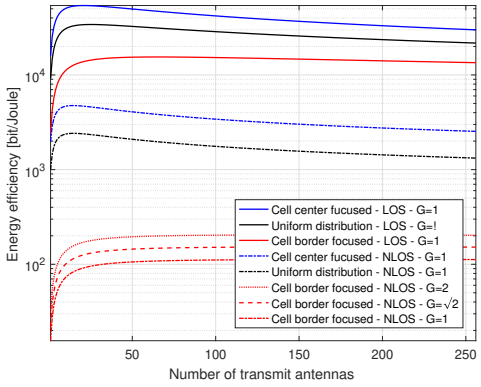

Fig. 2. Energy efficiency for three network topologies. The parameters used are: $\lambda_0 = 3$ [users/Km^2], $B = 12$, $\alpha = 2, 3$ (LOS, NLOS), $G = 1$.

- $P_{\text{PA}} = 5$, $P_0 = 1$, $P_{\text{common}} = 50$ [W].
- $P_{\text{RF}} = P_{\text{DAC}} + 0.5 < 1.5$ [W].
- $B \in [4, 12]$, $C_L = 12$ [pF], $\beta = 0.2$.

These values (except in the case of new parameters) are taken from [10] and [15] to keep consistency, ease comparison, and for tractability purposes.

We assume an OFDM modulated signal with $N = 2048$ active carriers, and a path-loss model for mm-waves as described in (8) at an operation frequency of 29 GHz, considering a distance $d < R = 200$ m between the UEs and the BS, distributed according to equation (5). For the propagation parameters, we consider $\bar{\alpha}_{\text{LOS}} = 2$, $\bar{\alpha}_{\text{NLOS}} = 3$ and $\bar{\sigma}_{x,\text{LOS}} = 4.5$, $\bar{\sigma}_{x,\text{NLOS}} = 8.5$, taken as the average values of the table in [12] for LOS and NLOS conditions, respectively. We model the PAPR as the maximum value of the threshold λ such that the probability $Pr\{\text{PAPR} > \lambda\} = 1 - [1 - e^{-\lambda}]^N < 1 \times 10^{-7}$ [14]. This leads to a PAPR of 13.8 dB for the OFDM signal. We also consider that this PAPR can be reduced from 3 to 6 dB with an adequate PAPR reduction technique, and thus $\sqrt{2} < G < 2$.

Figures 1 and 2 show the sum capacity and EE for the three considered user location distributions, under both LOS and NLOS conditions. As expected, they are both higher for the LOS channel. However, a large drop is observed for the

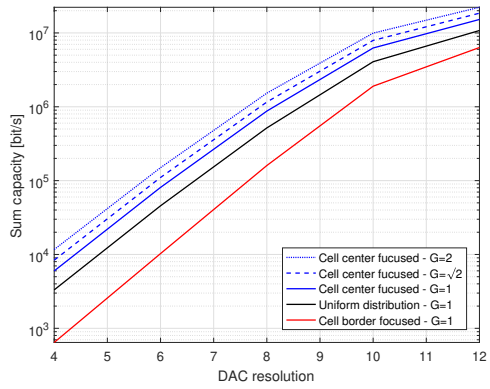

Fig. 3. Sum capacity as a function of DAC resolution. The parameters used are: $\lambda_0 = 3$ [users/km^2], $N_T = 64$, $\alpha = 2$, $G = 1$.

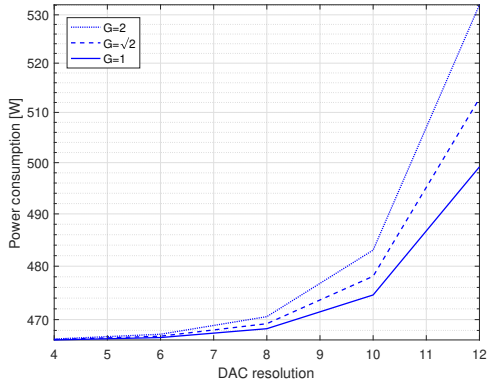

Fig. 4. Power consumption as a function of DAC resolution. The parameters used are: $\lambda_0 = 3$ [users/km^2], $N_T = 64$, $\alpha = 2$, $G = 1, \sqrt{2}, 2$.

case of NLOS with user location distribution near the cell border, which was not expected. Thus, the performance of an EE aware resource allocation scheme evaluated in this scenario largely underestimates the true performance in more realistic scenarios. It can also be seen that adding PAPR reduction indeed helps to raise both sum capacity and EE. This is shown only for NLOS channel with UEs near the cell border for readability, but the improvement is similar in all cases and consistent with [10].

Figures 3 and 4 show the sum capacity and power consumption as a function of DAC resolution for three PAPR levels. Again, Figure 3 highlights the deviation form the practical setups and the pessimistic case where all users are at the cell edge. There, it can be seen that the DAC resolution has a significant impact on sum capacity, due to the increment in SQNR. In addition, the associated higher power consumption (even greater with PAPR reduction) has a negligible effect on the total power for $B \leq 10$. Finally, for resolutions greater than 10 bits, the channel noise becomes dominant and the sum capacity curve flattens.

V. Conclusions

A model for the EE in massive MIMO systems has been proposed, considering the effect of PAPR reduction and DAC resolution for different user location distributions. The inhomogeneous PPP model allows to obtain results that accurately match the behavior in realistic deployments. We found that the pessimistic assumption of all users located at the cell edge leads to a large underestimation of the achievable energy efficiency of the system. Additionally, the analysis of the trade-offs raised by the effect of different DAC resolutions on power consumption, SQNR, and PAPR results a valuable tool for optimizing the systems design. DAC resolutions higher than 10 bits increase the power consumption without a significant gain in sum capacity. Although PAPR reduction also increases the power consumption, this increment can be kept low for DAC resolutions lower than 10 bits.

References

[1] ETSI, "5G NR Physical channels and modulation," standard, ETSI TS 38 211 V15.2.0 Technical Specification, 2018.

[2] S. Parkvall, E. Dahlman, A. Furuskar, and M. Frenne, "NR: The new 5G radio access technology," *IEEE Communications Standards Magazine*, vol. 1, pp. 24–30, Dec 2017.

[3] E. G. Larsson, O. Edfors, F. Tufvesson, and T. L. Marzetta, "Massive MIMO for next generation wireless systems," *IEEE Communications Magazine*, vol. 52, pp. 186–195, February 2014.

[4] T. S. Rappaport, S. Sun, R. Mayzus, H. Zhao, Y. Azar, K. Wang, G. N. Wong, J. K. Schulz, M. Samimi, and F. Gutierrez, "Millimeter wave mobile communications for 5G cellular: It will work!," *IEEE Access*, vol. 1, pp. 335–349, 2013.

[5] M. M. Molu, P. Xiao, M. Khalily, K. Cumanan, L. Zhang, and R. Tafazolli, "Low-complexity and robust hybrid beamforming design for multi-antenna communication systems," *IEEE Transactions on Wireless Communications*, vol. 17, pp. 1445–1459, March 2018.

[6] A. Elshafiy and A. Sampath, "Beam broadening for 5G millimeter wave systems," in *2019 IEEE Wireless Communications and Networking Conference (WCNC)*, pp. 1–6, April 2019.

[7] K. N. R. S. V. Prasad, E. Hossain, and V. K. Bhargava, "Energy efficiency in massive MIMO-based 5G networks: Opportunities and challenges," *IEEE Wireless Communications*, vol. 24, no. 3, pp. 86–94, 2017.

[8] C. A. Schmidt, M. Crussière, and J. F. Hélard, "Digital beamforming with PAPR reduction: An approach for energy efficient massive MIMO," in *91st Vehicular Technology Conference VTC2020-Spring*, May 2020.

[9] C. Schmidt, M. Crussiere, J. F. Helard, and A. Tonello, "Improving energy efficiency in massive MIMO: Joint digital beam-steering and TR-PAPR reduction," *IET Communications*, May 2020.

[10] C. A. Schmidt, J. F. Hélard, and M. Crussière, "Joint beamforming and PAPR reduction in massive MIMO: Analysis of gain in energy efficiency," in *2020 16th International Conference on Wireless and Mobile Computing, Networking and Communications (WiMob)*, pp. 1–6, 2020.

[11] O. Georgiou, C. Psomas, C. Skouroumounis, and I. Krikidis, "Optimal non-uniform deployments of LoRa networks," *IEEE Wireless Communications Letters*, vol. 9, no. 11, pp. 1919–1923, 2020.

[12] V. Raghavan, A. Partyka, A. Sampath, S. Subramanian, O. H. Koymen, K. Ravid, J. Cezanne, K. Mukkavilli, and J. Li, "Millimeter-wave mimo prototype: Measurements and experimental results," *IEEE Communications Magazine*, vol. 56, no. 1, pp. 202–209, 2018.

[13] B. Razavi, "The current-steering DAC [A circuit for all seasons]," *IEEE Solid-State Circuits Magazine*, vol. 10, no. 1, pp. 11–15, 2018.

[14] F. Gregorio, G. González, C. A. Schmidt, and J. Cousseau, *Signal Processing Techniques for Power Efficient Wireless Communication Systems: Practical Approaches for RF Impairments Reduction*. Signals and Communication Technology, Springer International Publishing, 2019.

[15] S. Han, C. I, Z. Xu, and C. Rowell, "Large-scale antenna systems with hybrid analog and digital beamforming for millimeter wave 5G," *IEEE Communications Magazine*, vol. 53, pp. 186–194, January 2015.